Putting things into perspective: Which visual cues facilitate automatic extraretinal symmetry representation? [A Registered Report]

Elena Karakashevska[1], Marco Bertamini[2], Alexis D.J. Makin[1]

[1]Institute of Population Health, University of Liverpool
[2]Department of General Psychology, University of Padova

Abstract

Introduction: Objects often project different images when viewed from different locations. Our visual system can correct for perspective distortion and identify objects from different viewpoints that change the retinal image. This study attempted to determine the conditions under which the visual system spends computational resources to construct view-invariant, extraretinal representations. We focused on extraretinal representation of planar symmetry. Given a symmetrical pattern on a plane, symmetry in the retinal image is degraded by perspective. Visual symmetry activates the extrastriate visual cortex and generates an Event Related Potential (ERP) called Sustained Posterior Negativity (SPN), and previous studies have found that the SPN is reduced for perspective symmetry during secondary tasks. However, we hypothesised that this **perspective cost** might be reduced when additional visual cues support extraretinal representation.

Method: 120 participants viewed symmetrical and asymmetrical stimuli presented in a frontoparallel or perspective view. The task did not involve symmetry, participants were instructed to discriminate the luminance of the patterns. Participants completed four blocks. In the **Baseline** block there were no cues supporting 3D interpretation. In the **Monocular** viewing block, participants viewed the same stimuli with one eye. In the **Static frame** block, additional pictorial depth cues were available - the elements appeared within a flat square surface with salient edges. In the **Moving frame** block, motion parallax was used to enhance 3D interpretation before stimulus onset.

Results: We computed perspective cost as the difference between the frontoparallel SPN and the perspective SPN. Contrary to our pre-registered hypotheses, perspective cost was uniform across all four blocks.

Discussion: We conclude that these visual cues do not substantially reduce perspective cost and promote extraretinal symmetry representation. Our Stage 1 protocol and our predicted results can be found here https://osf.io/6uae2/.

Keywords: perception; symmetry; view invariance; event-related potentials; SPN

Introduction

Many animals are tuned to visual symmetry and use it to guide adaptive behaviours (Møller & Thornhill, 1998). Symmetry is also a gestalt grouping principle that aids grouping and figure-ground segmentation (Koffka, 1935; Wagemans et al., 2012). Many psychophysical studies have investigated symmetry perception in humans (Barlow & Reeves, 1979; Treder, 2010), while the brain response to symmetry has been studied extensively in the last 20 years (for recent reviews see Bertamini et al., 2018; Cattaneo, 2017; Makin et al., 2023). Functional MRI studies have found that visual symmetry activates a network of regions in the extrastriate cortex, centred on object sensitive areas V4 and the Lateral Occipital Complex (Keefe et al., 2018; Kohler et al., 2016; Sasaki et al., 2005; Tyler et al., 2005; Van Meel et al., 2019). The extrastriate symmetry response can also be measured with EEG (Höfel & Jacobsen, 2007; Jacobsen & Höfel, 2003; Makin et al., 2012; Martinovic et al., 2018, Tyson-Carr et al., 2021). Symmetrical and asymmetrical stimuli, like all visual stimuli, generate event related potentials (ERPs) at posterior electrodes. These ERP waves begin with the P1 and N1 components of the visual evoked potential (VEP). After the VEP, there is a persistent difference between the ERP generated by symmetry and the ERP generated by asymmetry. This late difference is called the 'Sustained Posterior Negativity' (SPN). SPN amplitude scales with the proportion of symmetry in symmetry plus noise displays (Figure 1, Makin et al., 2020) and with other features that determine perceptual goodness of the configuration (Makin et al., 2016). The SPN is comparable when participants are classifying stimuli in terms of symmetry, or in terms of a different stimulus dimension such as colour (Makin et al., 2013, 2020). Indeed, analysis of a database called the complete Liverpool SPN catalogue (https://osf.io/2sncj/) suggests that symmetry is processed automatically whenever it is present in the retinal image (Makin et al., 2022). The current work investigates SPN responses to stimuli seen from perspective viewpoints, which distort symmetry in the retinal image. Such extraretinal symmetry might not be processed automatically.

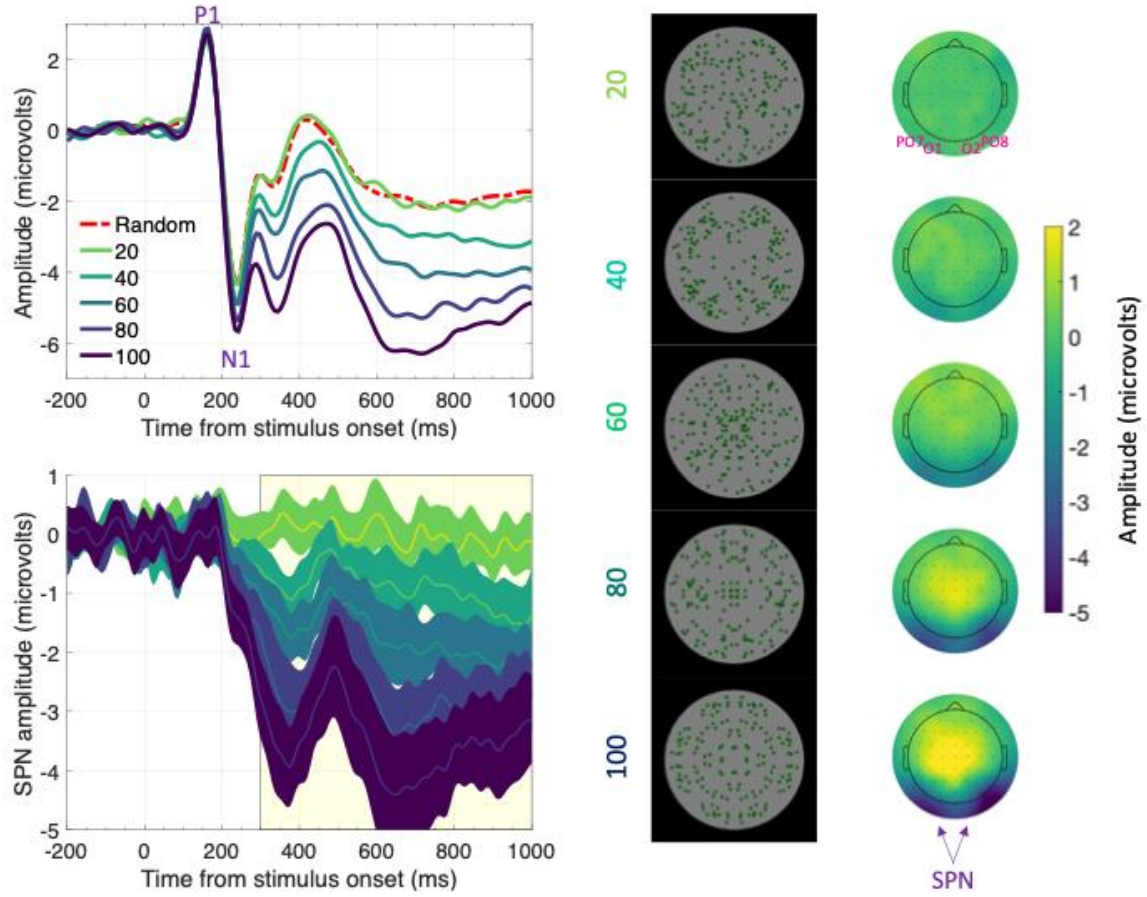

Figure 1. Results of Makin et al. (2020). The grand-average ERPs are shown in the upper left panel and difference waves (reflection-random) are shown in the lower left panel. A large SPN is a difference wave that falls a long way below zero. Topographic difference maps are shown on the right, aligned with the representative stimuli. The difference maps depict a head from above, and the SPN appears as dark blue at the back. Red labels indicate electrodes used for ERP waves [PO7, O1, O2 and PO8]. Note that SPN amplitude increases (that is, becomes more negative) with the proportion of symmetry in the image. In this experiment, the SPN increased from ~0 to –3.5 microvolts as symmetry increased from 20% to 100%. Figure adapted from Makin et al. (2022).

Retinal and extraretinal symmetry

The extrastriate symmetry network responds whenever symmetry is present in the retinal image. However, from an ecological standpoint, this is quite a rare scenario. Symmetrical objects only project a symmetrical image onto the retina when they are presented in the frontoparallel plane (Sambul et al., 2013; Sawada & Pizlo, 2008, Farshchi et al., 2021, Sawada & Farshchi, 2022). During naturalistic viewing, symmetrical objects are often seen from angles that distort retinal symmetry. We can often recognize that these objects are symmetrical, despite the perspective distortion. Terminology can vary in this field: We could say the visual

brain constructs a view-invariant representation of the symmetrical object, or alternatively we could say that it constructs a post-constancy representation or an allocentric representation. In this paper, we use the term 'extraretinal representation'.

The construction of extraretinal representations feels subjectively effortless. For instance, the rim of a coffee cup is perceived as circular, even when it projects an oval on the retinal image. It takes artistic training to draw an optically correct 2D image of a cup (with an oval rim), because an extraretinal representation of the 3D object (with circular rim) inevitably interferes (Thouless, 1933). The modern world frequently requires 2D shape constancy, although this subcase was probably less essential for our distant ancestors. For instance, we must recognize 2D letters on a printed page when holding a book at various angles. When driving, we can recognize 2D symbols on road signs from different angles and distances. We rarely notice any conspicuous change in the 2D shapes printed on planar surfaces, like pages and road signs, even when the retinal image changes dramatically. Like the majority of experiments in this field, we focused on extraretinal representations of 2D planar symmetry, rather than volumetric 3D symmetrical objects.

In many psychophysical studies on symmetry perception, participants discriminate between symmetrical and asymmetrical stimuli. Performance is impaired by perspective distortion (Bertamini et al., 2022; Koning & Wagemans, 2009; Locher & Smets, 1992; Szlyk et al., 1995; van der Vloed et al., 2005). The magnitude of this **perspective cost** varies between studies, partly depending on stimuli used and partly depending on the number of cues available. For instance, Szlyk et al. (1995) found that when stereo depth information specified surface angle, symmetry discrimination performance was nearly equivalent for frontoparallel and perspective displays. The authors note that interdependency is common in visual perception: The outcome of one perceptual operation (symmetry detection) depends on the outcome of another (surface angle determination). In the real world, there are often multiple perceptual cues to aid surface angle determination. Perspective cost may thus be smaller in many naturalistic viewing conditions than it is in typical lab studies with impoverished stimuli.

Neuroimaging studies suggest that the brain response to frontoparallel symmetry is automatic: It occurs whatever the participants' task. Meanwhile the brain response to perspective symmetry is more fragile and task dependent (Keefe et al., 2018; Makin et al., 2015; Rampone et al., 2019). Results from one key SPN study are shown in Figure 2. Here, Makin et al. (2015) compared SPN responses to frontoparallel and perspective symmetry,

which had a slant of +/-50 degrees around the vertical axis (Figure 2A). One group of participants classified the stimuli according to regularity (symmetry or asymmetry). Another group classified according to colour (light red or dark red). When participants were classifying by regularity, there was no perspective cost. The brain apparently achieved frontoparallel-perspective SPN equivalence during this regularity task (Figure 2B). Conversely, when participants classified the stimuli by colour, SPN amplitude was reduced in the perspective condition (Figure 2C).

Keefe et al. (2018) found comparable results with fMRI, and Rampone et al. (2019) found conceptually similar results in a different SPN study where symmetry was absent on the retina. Stereo defined symmetry is another form of extraretinal symmetry: Here symmetry is not present in the retinal image in each eye, and the cyclopean contours can only be seen when images are fused in the visual cortex. However, SPN amplitude is equal for stereo and contrast defined symmetry when participants perform symmetry discrimination tasks (Karakashevska et al., 2021).

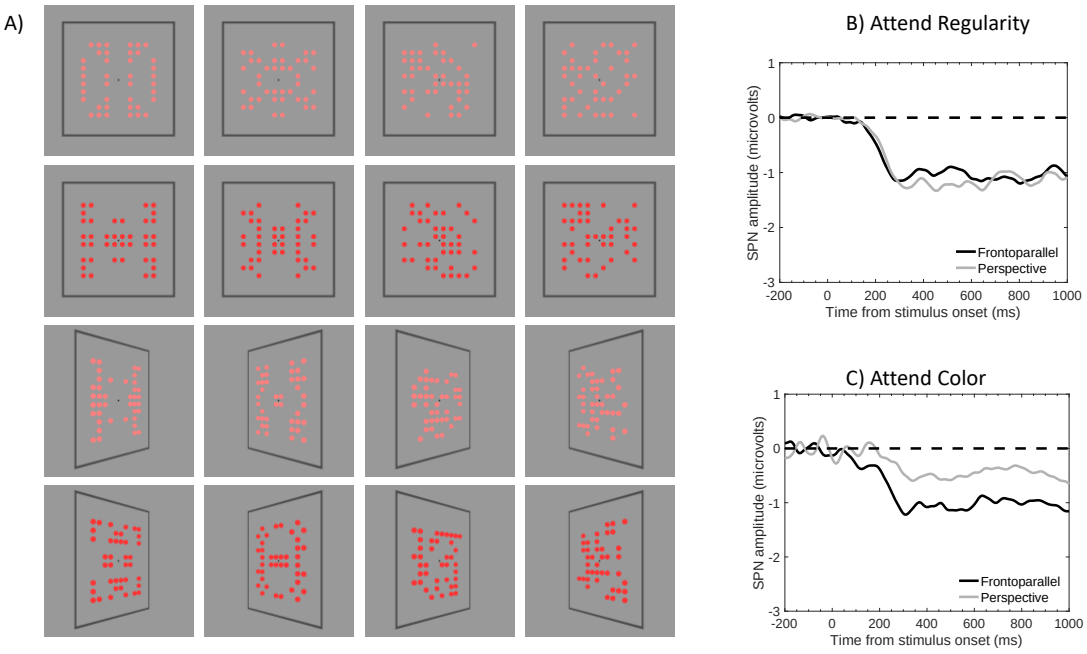

Figure 2. Stimuli and results of Makin et al. (2015). (A) examples of stimuli from a frontoparallel and perspective view. Participants either discriminated regularity (symmetry or asymmetry) or colour (light or dark red). **(B)** Grand-average SPN waves in the frontoparallel and perspective conditions of the regularity discrimination task. The SPN was similar in both

conditions. **(C)**. Grand-average SPN waves in the frontoparallel and perspective conditions of the colour discrimination task. The SPN was reduced in the perspective condition.

In sum, previous work suggests that extraretinal symmetry representations are not constructed automatically during secondary tasks. However, this contrasts with the apparent effortlessness of shape constancy. In our new study, we investigated whether extraretinal representations of symmetry can be constructed automatically during secondary tasks when sufficient cues are available to support 3D interpretation. We ran an experiment like the colour task in Makin et al. (2015) and systematically varied the number of cues available to support 3D interpretation. We expected that inclusion of additional cues would reduce perspective cost and make frontoparallel and perspective SPNs more similar (as they are in Figure 2B).

First, removal of cue conflict could reduce perspective cost (Stevens & Brookes, 1988, Vishwanath & Hibbard, 2013). Cue conflict happens when pictorial cues, like linear perspective and foreshortening, indicate that a surface is slanted in depth, while binocular stereo cues indicate that it is frontoparallel (Allison & Howard, 2000). Under monocular viewing conditions, cue conflict is eliminated, and participants are better at reporting depicted surface angle (Cornilleau-Pérès et al., 2002).

Second, additional pictorial depth cues could reduce perspective cost during binocular viewing (Li & Zaidi, 2004; Szlyk et al., 1995). The visual system may apply simplicity constraints – where the distorted shape (e.g., a lozenge) is always interpreted as a simple shape (e.g., a square) in perspective (Occam's razor principle; Pizlo, 2001).

Third, motion can also be used to reduce perspective cost (Welchman, 2016, Treue et al., 1996, Norman et al., 2004). The visual brain typically assumes that a changing retinal image is caused by a rigid object moving in 3D space, rather than plastic deformation of a 2D shape (Hoffman, 1998). In the real world, retinal motion is often caused by self-motion around a static object.

Previous behavioural studies have found that perspective cost may be reduced for polygons compared to dot patterns (Sawada & Pizlo, 2008, Wagemans, 1993). In a recent SPN study (Karakashevska et al., forthcoming), we found that polygons slightly reduce perspective cost but do not eliminate it. In the current work, we used dot patterns and acknowledge that the results may not generalize to polygons.

Study aims and hypotheses

We ran a within subject's experiment with four blocks. These blocks are termed (1) Baseline, (2) Monocular viewing, (3) Static frame, (4) Moving frame. In every block, participants discriminated between light and dark elements. We computed the SPN and the perspective cost in each block. The SPN is the difference between the symmetry and asymmetry wave, averaged over an interval from 300 to 600 ms post stimulus onset. In each block, we obtained a frontoparallel SPN (symmetry frontoparallel – asymmetry frontoparallel) and a perspective SPN (symmetry perspective – asymmetry perspective)[1]. The difference between frontoparallel and perspective SPNs is perspective cost. If the brain coded frontoparallel and perspective stimuli as nearly equivalent, perspective cost would be nearly zero (as in Figure 2B). This would indicate that the visual manipulations are sufficient for perfect extraretinal representation.

Our predicted results are shown in Figure 3. We predicted that perspective cost would be highest in the Baseline block, where there are no cues supporting extraretinal representation of symmetry. We predicted a reduction in perspective cost in the Monocular viewing block, where cue conflict was removed by covering one eye. We also predicted a reduction of perspective cost in the Static frame condition, where a static frame is available for 2.5 seconds before stimulus onset. We also predicted a further reduction of perspective cost in the Moving frame block, where the frame is seen to rotate through 20 degrees before stimulus onset, supporting 3D interpretation. Given the results of Makin et al. (2015) and Karakashevska et al. (forthcoming), we predicted perspective cost to be around 1 microvolt in the Baseline block, and then reduced by 0.5 microvolts with each additional cue, and it would thus reach zero in the Moving frame block, where frame and motion cues summate.

[1] In several places the word 'random' was used in the In Principle Acceptance Stage 1 submission. We have changed this to 'asymmetry' in the Stage 2 submission for consistency.

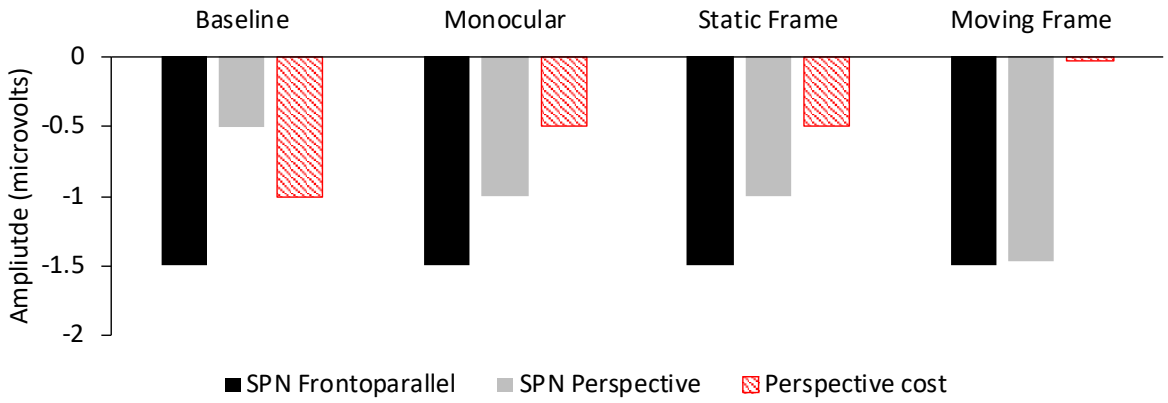

Figure 3. **Predicted results.** The SPN is the difference between symmetrical and asymmetrical conditions (negative bars represent a large SPN). The SPN may be larger (more negative) in frontoparallel (black) than perspective (grey) conditions. This difference is called **perspective cost** (red). We predicted that perspective cost would be highest in the baseline block (left) and reduced in the other three blocks. Perspective cost may approach zero in the moving frame block (right). The predicted amplitude of these effects is more speculative than the rank order.

The above can be listed as three specific hypotheses (as outlined in Table 1). Hypotheses 1 and 2 state plausible background assumptions. Hypotheses 3 and 4 are of key theoretical interest.

Hypothesis 1

In the frontoparallel conditions amplitude will be lower for symmetry compared to asymmetry at posterior electrodes between 300 and 600 ms post stimulus onset. We were confident that this SPN would be found given the number of previous studies with similar frontoparallel stimuli (Makin et al., 2022).

Hypothesis 2

In the Baseline block, SPN will be substantially larger (more negative) for frontoparallel than perspective stimuli. In other words, perspective cost will be substantial in the baseline block (Makin, 2015).

Hypothesis 3

Hypothesis 3 predicts perspective cost differences across the four blocks (red bars in Figure 3). This can be stated as four predicted pairwise differences:

a) Perspective cost will be reduced in the Monocular viewing block (as compared to Baseline).

b) Perspective cost will be reduced in the Static frame block (as compared to Baseline).

c) Perspective cost will be reduced in the Moving frame block (as compared to Baseline).

d) Perspective cost will be reduced in the Moving frame block (as compared to Static frame block).

Hypothesis 4

Perspective cost will approximate zero in the Moving frame block only. In other words, we predict near-perfect frontoparallel-perspective SPN equivalence in the Moving frame block, and not in the other three blocks.

Method

The Stage 1 manuscript of this Registered Report (RR) has been formally registered on OSF after receiving in-principal acceptance (https://osf.io/6uae2/). The OSF project repository associated with this RR can also be found on OSF (https://osf.io/9pmrh/). The study had institutional ethics committee approval (Ref 11514) and was be conducted in accordance with the Declaration of Helsinki (revised 2008). Participants were recruited using convenience sampling and were compensated for their time with money or course credit. All the study information was provided and informed consent was obtained from all participants. Data collection and analysis was not performed blind to the conditions of the experiments.

Participants

We recruited a sample of 120 participants (24 male, 19 left-handed) between the ages of 18 and 43 (mean = 20.76, SD = $\pm$ 4.76). This allowed all 24 combinations of block orders to be presented 5 times. All participants had normal or corrected to normal vision and no history of neurological conditions, as per a self-report. For the monocular viewing condition in the experiment, the preferred sighting eye of participants was determined in the lab, using the hole-in-the card test. A red cross (3 × 3 cm) was presented approximately 5 m in front of the

participant. The participant was instructed to hold a card (13 × 20 cm) with both hands, at arm's length and move the card until the cross is visible through a hole in the centre of the card (1.5 cm in diameter), with both eyes open. The experimenter then covered the right eye of the participant and asked if the cross has remained in his/her line of view. The eye that allowed the participant to maintain the view of the cross while the other eye is closed was documented as the preferred sighting eye. We found that 43 participants were left eye dominant.

Power analysis

We powered our experiment to find relatively small ERP differences of 0.35 microvolts. This threshold is informed by analysis of the 249 SPNs in the SPN catalogue (https://osf.io/2sncj/), described in Makin et al. (2022). Figure 4 illustrates relevant SPN distributions. Each ridge in Figure 4A represents a distribution of participant SPNs around the mean (the largest, most negative, SPN is at the base). The scatterplot in Figure 4B shows all 249 SPNs as data points, with mean amplitude on the X axis, and Cohen's d_z (Mean / SD) on the Y axis. The second order polynomial regression line indicates a plausible effect size d for an SPN of a given amplitude. This shows that -0.35 microvolt SPNs are likely to have Cohen's d_z of -0.34. This also applies to within-subject pairwise differences between SPNs.

Furthermore, as explained in Makin et al. (2022), 178 of the 249 SPNs in the catalogue are statistically significant ($p < 0.05$, one sample t test against zero, two-tailed). The smallest significant SPN in the catalogue is -0.342 microvolts. Our threshold of -0.35 microvolts is thus a reasonable a priori definition of a *small but meaningful* SPN or SPN modulation.

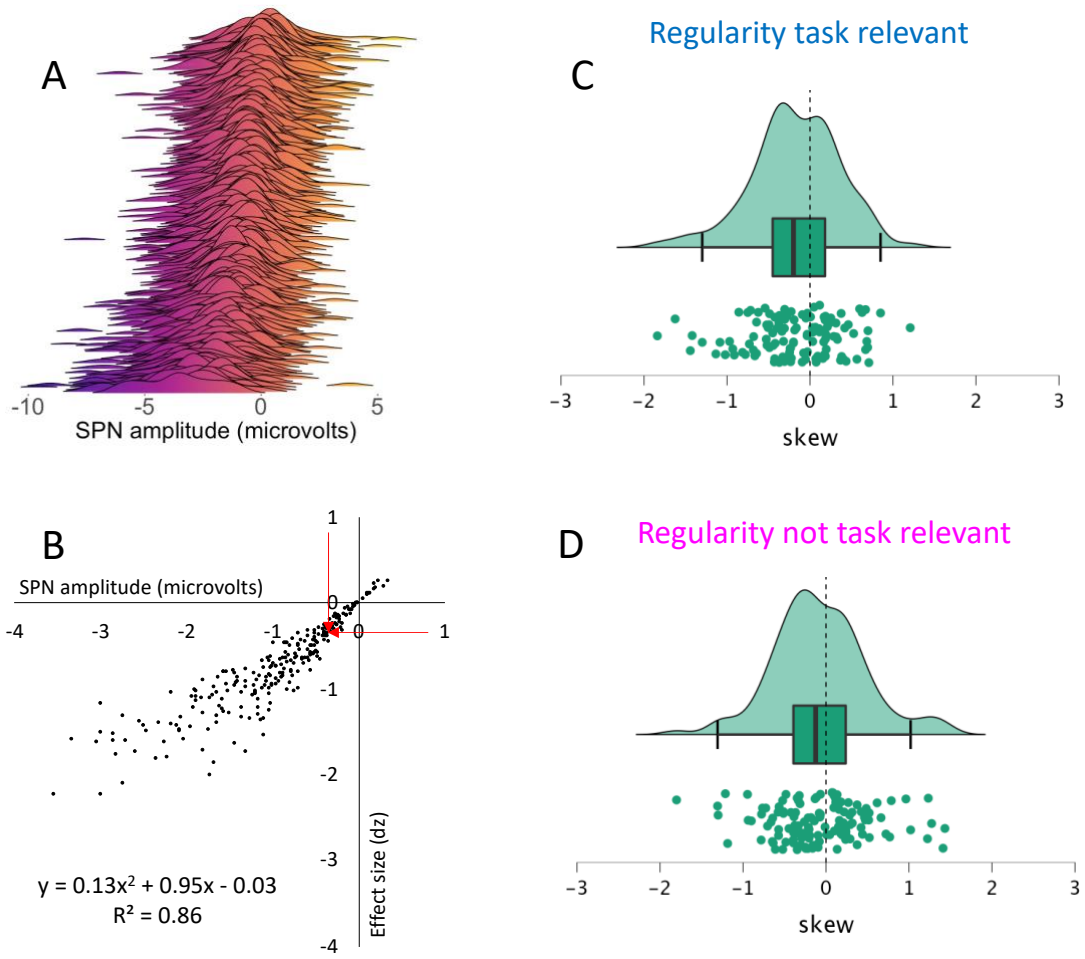

Figure 4. A) Distribution of 249 SPNs from the SPN catalogue (https://osf.io/2sncj/), shown as a ridgeplot. Each ridge is a distribution of individual participant SPNs around the mean. The largest (most negative) SPN is at the base. B) Scatterplot of 249 SPNs. The X axis is SPN amplitude in microvolts. The Y axis is standardized effects size (Cohen's d_z). The second order polynomial line suggests -0.35 microvolt SPNs have a typical effect size d of -0.34 (red arrows). C) Distribution of skewness statistics from experiments where regularity was task relevant. D) Distribution of skewness statistics from experiments where regularity was not task relevant.

We chose a sample size of 120. The most demanding part of our research, in terms of sample size, is testing the four pairwise perspective cost differences stated under hypothesis 3. N=120 gives 88% power to find significant pairwise differences with effect size d = 0.34, and with alpha = 0.0125. This conservative threshold of 0.0125 reflects a Bonferroni correction for 4 pairwise comparisons (0.05/4 = 0.0125). We applied the Bonferroni correction despite that fact we make a priori predictions, and we used two-tailed tests despite the fact these predictions were directional. By some conventions, one-tailed tests with no correction for familywise error rate would be justifiable, but we lean towards 'overpowering'

the study rather than missing real effects (Brysbaert, 2019). We also note that the median sample size in previous SPN research is just 24. Our sample of 120 is more than twice as large as any published or unpublished within-subjects SPN experiment. The sample of 120 is partly constrained by needs to balance block order (24 orders X 5 repeats of each). Sample size must be a multiple of 24, and N= 96 would be underpowered by these standards (power = 0.78, alpha = 0.0125, d = 0.34, two tailed) while N=144 exceeds our resources and time constraints.

We verified these decisions with a power simulation approach. We computed a power analysis on 10,000 observations from a bivariate normal distribution with a specified correlation of 0.5 between conditions. This confirms we have approximately 90% power of finding a mean pairwise difference of 0.34 SDs with a sample of 120 (codes for the simulations can be found here: https://osf.io/utq8e).

Hypothesis 4 predicts an absence of perspective cost in the Moving frame block. Here we used a one-sided equivalence testing approach (illustrated in Figure 8). If true perspective cost is -0.35 microvolts in a given block, we are likely to find that the effect is significantly *below* zero microvolts with one tailed one sample t test (power = 0.95, Cohen's d_z = 0.34, alpha = 0.02, one-tailed). Conversely, if true perspective cost is zero microvolts in given a block, we are likely to find the effect is significantly *above* -0.35 microvolts (power = 0.95, Cohen's d_z = 0.34, alpha = 0.02, one-tailed).

Normality assumptions

Indeed, only 8-9% of the 249 SPNs violate the assumption of normality according to Shapiro-Wilk and Kolmogorov-Smirnov tests ($p < .05$). However, median sample size in this analysis was just 24, and these tests will often miss departures from normality. Meanwhile, accepting normality based on $p > 0.05$ is a statistical fallacy of confirming the null hypothesis. We therefore analysed the distribution of 249 skewness statistics associated with the 249 SPNs. There is a small but significant mean negative skew when regularity is task relevant (Figure 4C, mean = -0.174 microvolts, SD = 0.529, t (124) -3.665, $p < .001$). However, this is less pronounced when regularity is not task relevant (Figure 4D, mean – 0.081 microvolts, SD = 0.561, t (123) = -1.609, p = .110). We can therefore assume that normality is a reasonable approximation of the population distribution.

Apparatus

Participants were positioned 57 cm from a 51 X 29 cm (1920 X 1080 pixel) HP E233 LED backlit monitor, with 60Hz refresh rate. A chin rest was used for gaze stabilization. EEG data was recorded continuously at 512 Hz from 64 scalp electrodes (BioSemi Active-2 system, Amsterdam, Netherlands). Horizontal and Vertical EOG external channels were used to monitor excessive blinking and eye movements. These channels were not included in analysis. Participants viewed the stimuli through an aperture covering the rectangular edges on the monitor. For the Monocular block, participants wore a gauze eyepatch to cover their non-dominant eye[2].

Stimuli

The stimuli were pre-generated and saved as .png files. This eliminated the computation involved in stimulus generation from the experiment itself and allowed precise control over stimulus timing. Stimuli were produced using open source PsychoPy software (Peirce, 2007). PsychoPy codes for generating the stimuli and running the experiments are available on OSF for peer review (https://osf.io/t2zwa).

Example stimuli are shown in Figure 5. The frontoparallel conditions are in the central column, and different levels of perspective slant (-/+ 60 degrees) and tilt (+/- 15 degrees) are in the left and right columns. Patterns without frames are shown in upper rows whilst patterns with frames are shown in lower rows. Several pictorial depth cues support 3D interpretation in the perspective conditions. The frame gives the impression that the elements are printed on a flat surface with salient edges. This is subject to salient foreshortening. The top and bottom edges of the frame converge on a vanishing point to the left or right, suggesting they are parallel in the object. The left and right edges also converge on a vanishing point far above or below, again suggesting they are parallel in the object. When there are horizontal and vertical symmetry lines, these converge on the same vanishing points as the frame. The size of the elements, and distance between them, also produces a mild texture gradient. Finally, elements are ovals, consistent with a circle seen in perspective.

[2] We mistakenly suggested this would always be the left eye in the In Principle Acceptance Stage 1 submission.

Similar stimuli have previously been found generate large SPNs in frontoparallel conditions. Meanwhile, an online behavioural study by Bertamini et al. (2022) used similar stimuli and found a significant perspective cost on response time during a symmetry/asymmetry discrimination task.

All patterns are arrangements of 40 Gaussian filtered dot elements in a square region (Figure 6A). In the frontoparallel conditions with frame, the frame is 6.6 X 6.6 cm, and thus 6.6 X 6.6 degrees of visual angle (dva). This has an implicit grid of 12 X 12 cells. During stimulus generation, the central 10 X 10 grid was populated with small dots (approximate 0.25 dva diameter, Figure 6). Each 5X5 cell quadrant had 10 dots (occupying 40% of the available 25 cells). In the first quadrant the occupied cells were chosen randomly. Within each occupied cell, dot location was jittered randomly on the X and Y dimensions, so they were rarely located at cell centre. This stopped the appearance of multi-element straight lines spanning several cells. Without jittering, asymmetrical patterns of have perfectly straight rows and columns of aligned elements. For symmetrical patterns, the first quadrant was reflected twice, giving horizontal and vertical reflection. For asymmetrical patterns, all four quadrants were generated independently. Symmetrical and asymmetrical stimuli were indistinguishable based on information in a single quadrant. These stimuli were recently used in a paper by Makin et al. (2024), which reported strong SPNs during a luminance task with frontoparallel presentation.

The luminance of the light and dark elements was chosen to ensure the task would be easy to perform (0.459 vs 8.680 cd/m^2). In a pilot experiment with these stimuli, luminance discrimination performance was above 90% correct. The grey shade behind the dots was identical in all blocks (47.97 cd/m^2), so the luminance discrimination task was equivalent. However, in the Static frame and Moving frame blocks, the screen background, behind the frame, was marginally darker than the frame region (41.69 cd/m^2). It was thus marginally darker than the same region in the Baseline and Monocular blocks. This feature was chosen to enhance the appearance of the frame region as a planar surface painted with dot elements.

Perspective views were produced by changing the position of a virtual camera on the surface of a virtual sphere, looking inwards towards the centre (Figure 6). The ‘equator’ of the sphere is horizontally aligned with the horizontal midline of the screen. The vertical ‘meridian’ of the sphere is aligned with the vertical midline of the screen. A stimulus in the middle of the screen has a centre point at the centre point of the virtual sphere. The sphere has a radius of

57cm (the same as the distance the participant is from the screen in the experiment). For frontoparallel trials, the virtual camera was on the equator and vertical meridian – looking at screen centre. For perspective trials, the virtual camera moved around the equator by +/- 60 degrees, and up or down the meridian by +/- 15 degrees (see protractor diagram in Figure 5B). There are thus four possible perspective views ([-60, -15], [-60,15], [60, -15], [60,15]).

These perspective stimuli have several advantages over those used by Makin et al. (2015). In Makin et al. (2015), the position of the participant's eye and virtual camera were not matched (see Sawada & Pizlo, 2008 for more on importance of eye position). This is a limitation, because the participants in Makin et al. (2015) had to do two visual transformations, first adopting the position of the virtual camera, and then correcting for perspective distortion. Furthermore, symmetry around the vertical axis was not substantially disrupted by the perspective in Makin et al. (2015). This feature can be seen by inspecting the stimuli in Figure 2. Consequently, if participants focused spatial attention on the axis region, they would have near-perfect retinal symmetry to guide judgements. In the new study, slant and tilt were used to reduce retinal symmetry around the axis. The angles of 60 and 15 degrees were chosen for consistency with previous work (same as Karakashevska et al., forthcoming, and the centre of the slant range used by Sawada and Pizlo, 2008).

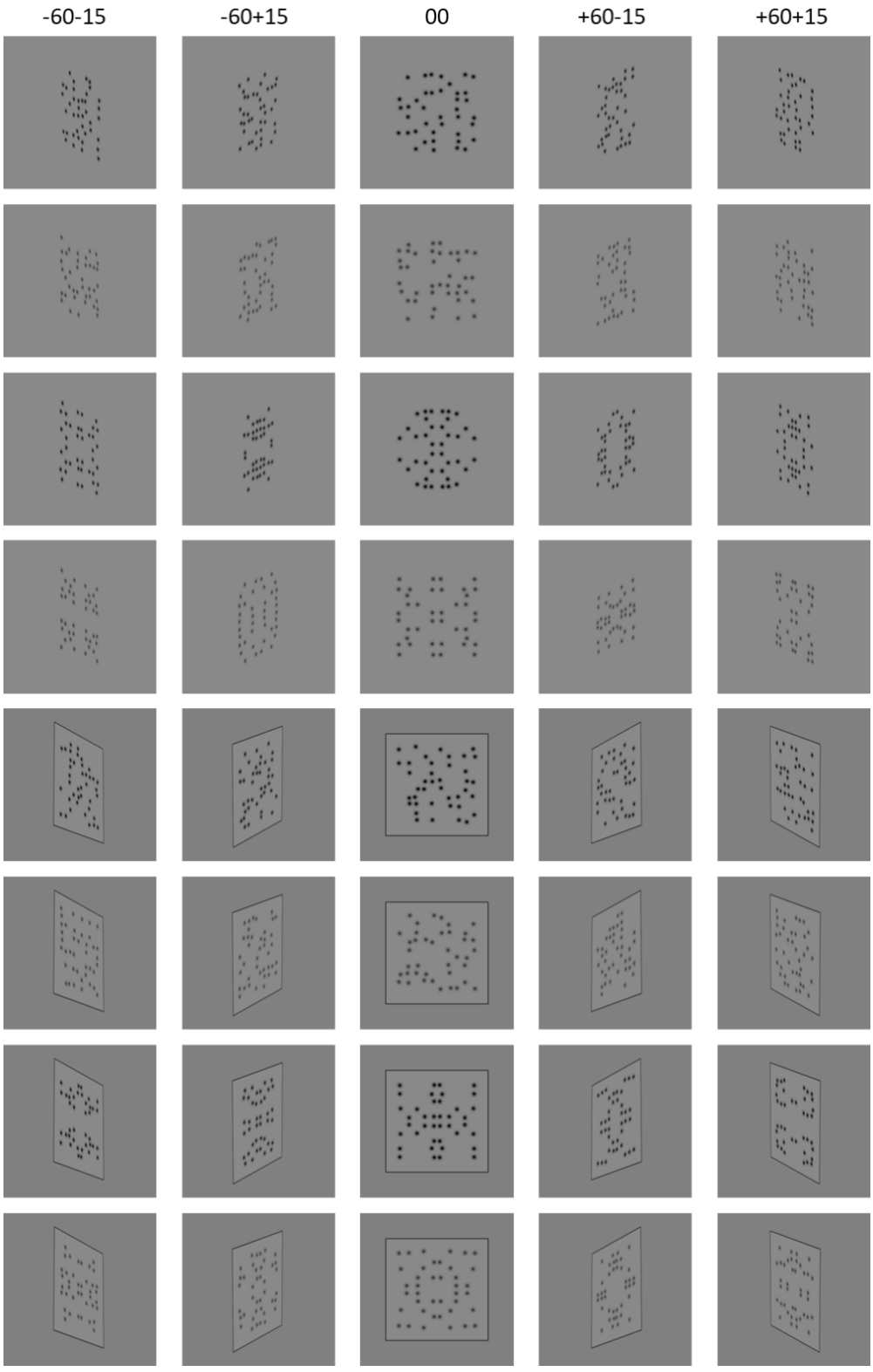

Figure 5. Example stimuli for each possible combination of regularity, angle, and luminance. The frontoparallel conditions are in the central column, and different levels of slant (-/+ 60 degrees) and tilt (+/- 15 degrees) are to the left and right. Patterns without frames are shown in upper rows (used in Baseline and Monocular blocks). Patterns with frames are shown in lower rows (used in Static and Moving frame blocks).

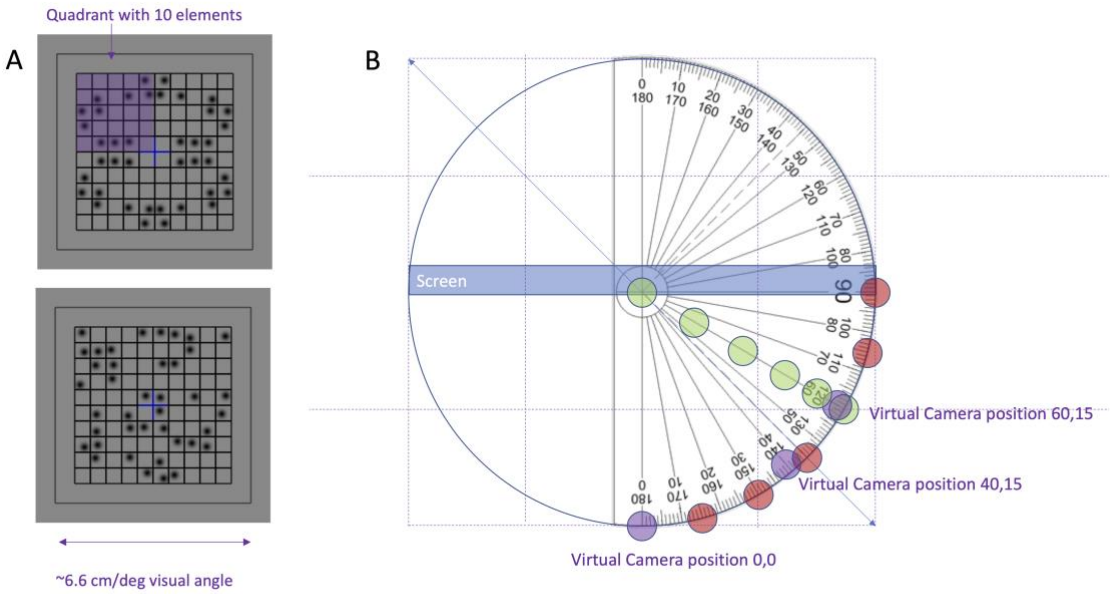

Figure 6. Stimulus construction diagram. A) Arrangement of dots in symmetrical and asymmetrical exemplars. The top panel shows construction of a symmetrical exemplar. A quadrant is populated with 10 small Dot elements (highlighted in purple). This quadrant was reflected across horizontal and vertical axes. The bottom panel shows construction of an asymmetrical exemplar. Here all 4 quadrants are independent. B) The protractor diagram represents virtual view angles used to generate perspective stimuli. This is a top-down view of a screen. The centre of the screen is in the centre of a virtual sphere. The protractor represents the equator of this sphere. Purple dots are virtual camera positions used in stimulus rendering. The camera is always focused on the centre of the screen/sphere.

Procedure

The participants were first presented with the instructions for the experiment and were informed that the task was to classify dot element luminance.

There were four blocks in total (Baseline, Monocular, Static frame and Moving frame). This gives 24 possible block orders; 5 participants completed each order. There were 256 trials in each block, with 32 repeats in each of 8 conditions [(symmetry, asymmetry) X (frontoparallel, perspective) X (light, dark)]. Trials in each block were presented in a different randomized order for each participant. There were 15 breaks in each block where the experiment paused, and the experimenter could check the electrodes. Each block was preceded with an 8-trial practice with equivalent stimuli. The practice was used to acquaint participants with the key response mapping and luminance difference.

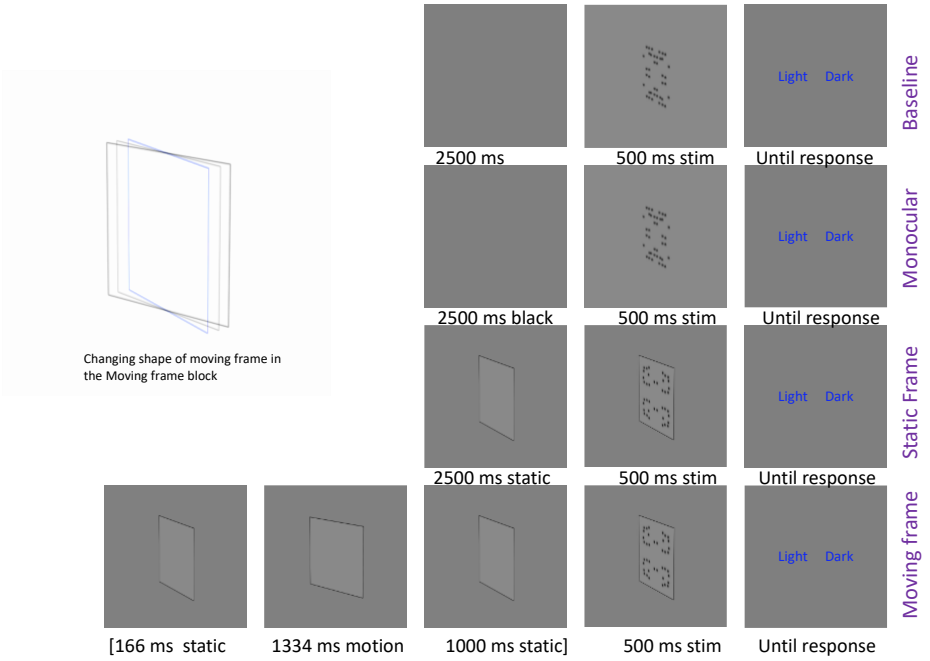

Figure 7. Trial structure in the 4 blocks. In the Baseline and Monocular blocks, each trial began with a 2500 ms blank screen. This was followed by a 500ms stimulus presentation and a response screen. In the Static frame and Moving frame blocks, each trial begins with an empty frame. In the Moving frame block, the virtual camera changes location during the first part of the pre-stimulus interval, giving the impression of a frame rocking back and forth around the vertical axis (see inset).

Trial structure is shown in Figure 7. The pre stimulus interval was 2500 ms, followed by a 500 ms stimulus presentation. The participant then entered their response in an unspeeded fashion after stimulus offset using the A and L keys of a standard keyboard. All trials gave feedback informing the participants when they entered the wrong answer (e.g., 'dark' on a light trial). In the baseline and monocular blocks, the 2500 ms pre stimulus interval was blank. In the Static frame and Moving frame blocks, the frames were presented for 2500 ms before stimulus onset. Frame orientation was consistent with the subsequent stimulus (so, for example, a -60-15 frame preceded a -60-15 stimulus). In the Moving frame block, the first part of the pre-stimulus interval showed a moving frame.

For the perspective conditions of the Moving frame block, the virtual camera moved round 20 degrees, from its most extreme starting position at +60 (or -60) degrees to position nearer the meridian at +40 (or -40) degrees and back again. Vertical position never changed, remaining at + or - 15 degrees (see inset in Figure 7). The camera shift happened twice, giving the perceptual impression that the frame rocks back and forth (diagrammatised with purple dots on the protractor in Figure 6). The final frame position was always +/- 60 degrees in the

perspective conditions. For the frontoparallel conditions of the Moving frame block, the frame moved from 0 to -/+ 20 degrees and back again twice. Motion to the left or right in the frontoparallel condition was equally likely and counterbalanced across other experimental conditions. The final 1000 ms of pre-stimulus interval displayed a static frame and was identical to the equivalent interval of the Static frame block. This feature was designed to avoid motion energy during the ERP epochs. The motion evoked potentials generated by the moving frame were completed long before the baseline period.

EEG data pre-processing

EEG data was processed offline using eeglab functions in MATLAB 2022b. The planned analysis pipeline (https://osf.io/vu2m7) was followed. This was very similar to other SPN studies. EEG data was recorded from 64 channels arranged according to the extended international 10-20 system. Offline data was referenced to scalp average, low pass filtered at 25 Hz (using the FIR filter pop_eegfiltnew function in eeglab2023.0), and down sampled to 256 Hz and segmented into -500 to 700 ms epochs with a -200 to 0 ms pre-stimulus baseline. Previous work has shown that low pass filter properties do not substantially distort the SPN signal, although high pass filtering can mask it (see supplementary materials of Makin et al. 2020). Eye blinks and other large artefacts were removed using Independent Components Analysis (ICA). ICA cleaning was automated based on the Adjust function in EEG lab (Mognon et al., 2011). Problematic channels were identified with a semi-automatic procedure and zeroed before ICA components were computed. This procedure involved a GUI with an amplitude plot where anomalous channels were identified visually through variance distributions. These channels will then be replaced with spherical interpolation. The average reference was recomputed after interpolation. After this, trials where amplitude exceeds +/- 100 microvolts were removed. Any participant with fewer than 50% of trials remaining on any block after these procedures was replaced.

The spatiotemporal cluster for SPN analysis was pre-determined. The time window used was 300-600 ms post stimulus onset. ERPs were computed from two electrode clusters [P3 P5 P7 P9 PO7 PO3 O1 (left); and P4 P6 P8 P10 PO8 PO4 O2 (right)]. We averaged amplitudes across time points, and then across electrodes, using the *stats extractor 2020.m* script (https://osf.io/vu2m7). This electrode cluster best captured the SPN in a previous study using similar perspective dot stimuli (Karakashevska et al., forthcoming). In each block, we

obtained a frontoparallel SPN (symmetry frontoparallel – asymmetry frontoparallel) and a perspective SPN (symmetry perspective – asymmetry perspective). Perspective cost was defined as the difference between frontoparallel and perspective SPNs.

Statistical data analysis plan

Prior to analysis of the ERP data, the behavioural performance on the luminance discrimination task was assessed. Any participants whose performance fell below 80% on any block was replaced. Given the results of Karakashevska et al. (forthcoming), we anticipated that most participants would be over 95% correct on this task.

For hypothesis 1 we tested for presence of an SPN in the frontoparallel conditions. We ran a 2 Regularity (Symmetry, Asymmetry) X 4 Block (Baseline, Monocular, Static frame, Moving frame) repeated measures ANOVA. We expected a strong main effect of Regularity.

For hypothesis 2, we tested for a difference between frontoparallel and perspective SPNs in the Baseline block. We used a two-tailed paired samples t test. We predicted the mean SPN to be larger (i.e., more negative) in the frontoparallel condition.

For hypothesis 3 our dependant variable was perspective cost (frontoparallel SPN – perspective SPN). We predicted 4 pairwise differences between blocks: perspective cost reductions in each block compared to the baseline, and a perspective cost reduction in the Moving frame block compared to Static frame block (Figure 3). These four differences were tested with four two-tailed paired samples t tests. Alpha level was adjusted to correct for multiple comparisons (0.05/4 = 0.0125).

Hypothesis 4 predicted that meaningful perspective cost would be eliminated in the Moving frame block. This was different from other hypotheses because we predicted absence of an effect. We thus used a one-sided equivalence testing approach. Perspective cost in the Moving Frame block was predicted to be significantly above -0.35 microvolts (our definition of a small negative ERP effect). Significance was established with one-tailed, one sample t tests.

Results

Behavioural data results

Participants correctly discriminated light from dark dots on most trials in all blocks (Figure 8A). Five participants who fell short of the 80% criteria in at least one block were replaced.

There was a significant difference across Blocks with a non-parametric Friedman's Test (χ^2 (3) = 72.417, p < .001, Kendall's W = .201, Figure 8A). Non-parametric Wilcoxon signed ranks tests found that pairwise differences all pairwise differences were significant (p < 0.044) except Frame vs. Moving frame (p = 0.155, Figure 8B). However, the difference between blocks was small in absolute terms, with means between 94 to 97% correct.

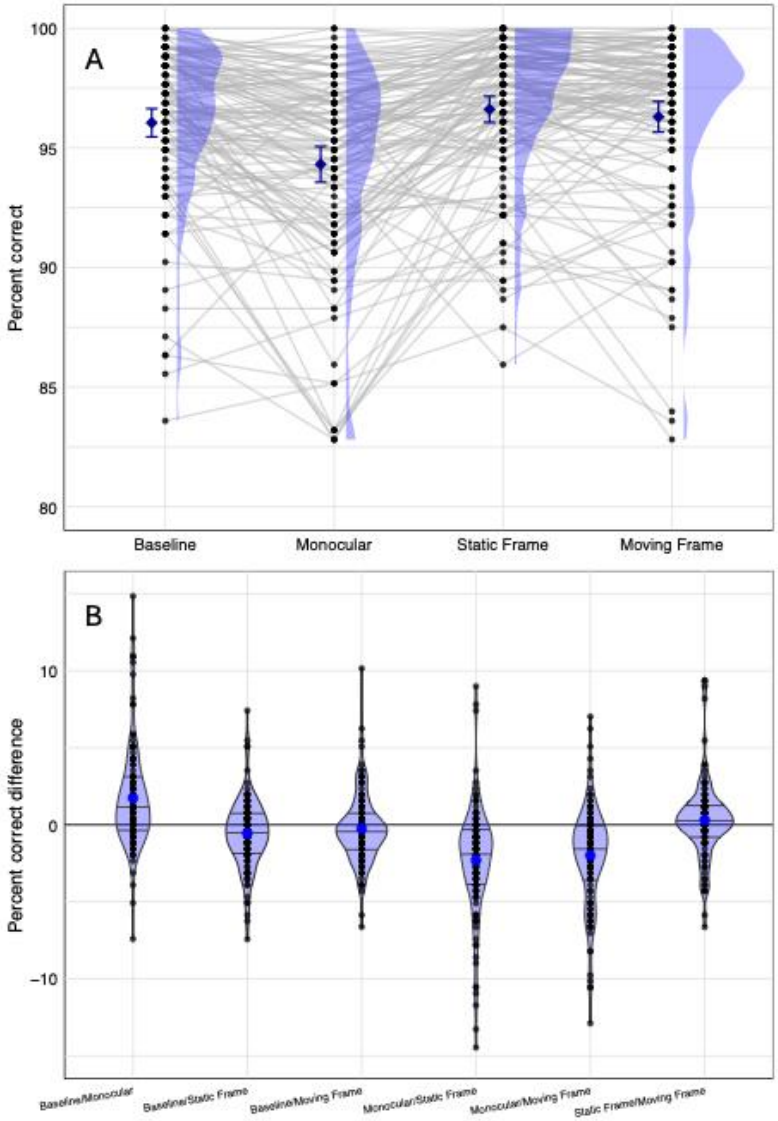

Figure 8. Scatterplot of the behavioural results and distribution of pairwise differences. A) a scatterplot showing paired observations with half eye density plots showing the distribution on the right-hand side, and the mean with error bars of 95% CI. There are many overlapping dots, so we do not see 120 data points. B) The distribution of the pairwise differences using violin plots.

EEG data pre-processing outcomes

The number of ICA components removed in different blocks were as follows: Baseline (M = 5.58, min = 1, max = 22); Monocular (M = 5.65, min = 1, max = 28); Static frame (M = 5.99, min = 1, max = 35); Moving Frame (M = 5.87, min = 0, max = 26).

The number of interpolated channels were as follows: Baseline (37 participants had at least one channel interpolated, max = 3); Monocular (48 had at least one, max = 2); Static frame (45 had at least one, max = 3); Moving frame (41 had at least one, max = 3).

Trial inclusion rates in percentages were as follows: Baseline (M = 95.6%, min = 55.5%, max = 100%); Monocular (M = 96.8%, min = 53.5%, max = 100%); Static frame (M = 95.9%, min = 67.6%, max = 100%); Moving Frame (M = 96.5%, min = 75.4%, max = 100%). Seven participants that did not meet the a priori 50% minimum trial inclusion criteria and were replaced.

Sustained posterior negativity

ERPs are shown in Figure 9 and 10, and topographic difference maps are shown in Figure 11. All conditions generated an SPN (symmetry – asymmetry < 0). SPN amplitude was reduced in the perspective conditions. Contrary to predictions, this perspective cost was similar in all blocks.

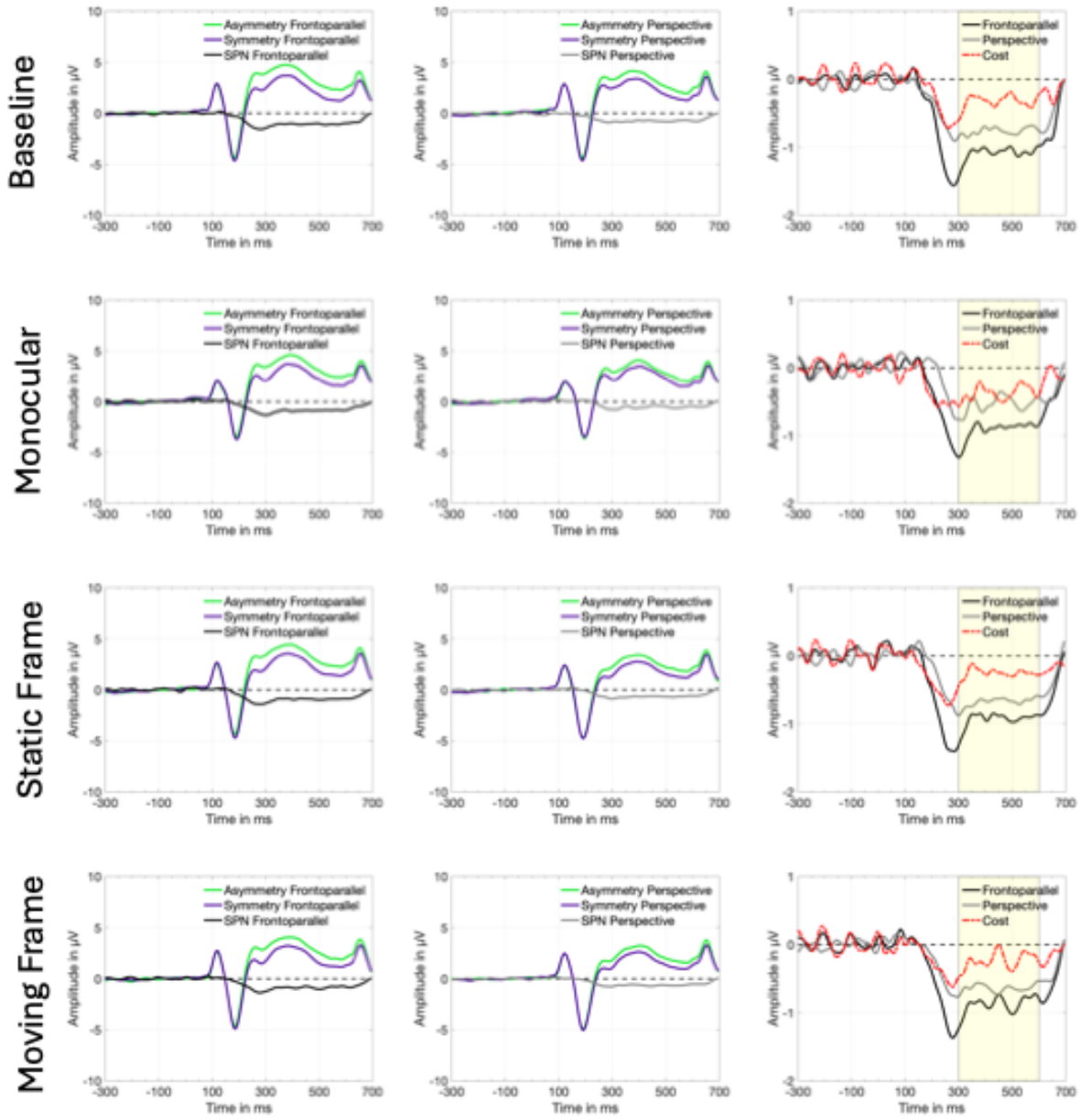

Figure 9. ERPs from the posterior electrode cluster. Rows correspond to blocks. The leftmost column illustrates the ERP waves for frontoparallel asymmetry (green) and frontoparallel symmetry (purple) with the symmetry-asymmetry difference superimposed (grey). The central column illustrates the same data for the Perspective conditions. The rightmost column presents the SPN and perspective cost as difference waves. The SPN was consistently larger (more negative) for frontoparallel (black) compared to perspective (grey) presentations, with a similar perspective cost observed across all four blocks (red). The 300-600 ms interval used in statistical analysis is highlighted (yellow).

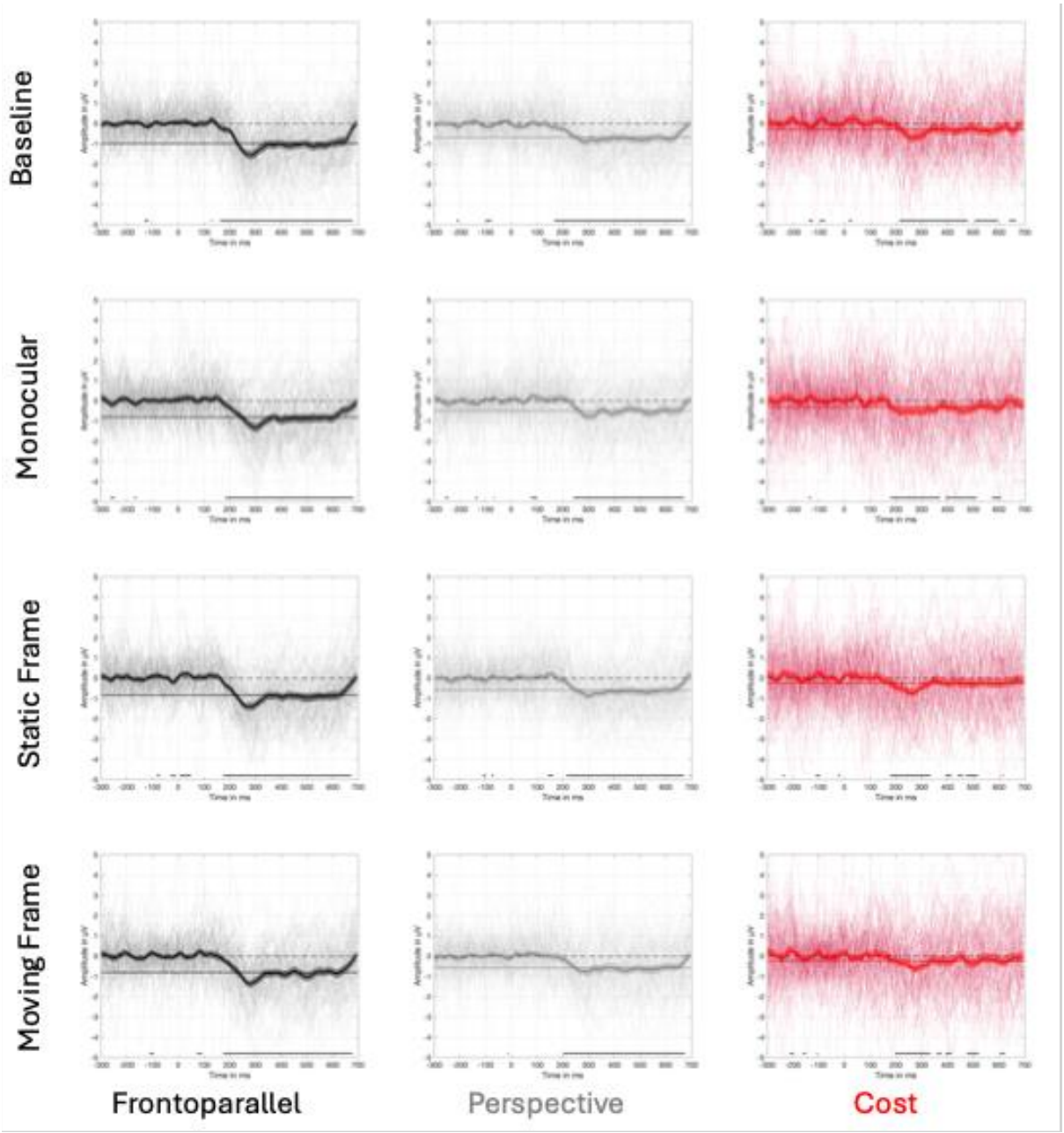

Figure 10. Difference waves with interparticipant variance. Difference waves are illustrated with a solid line, superimposed on the 95% CI ribbon. Differences from individual participants are shown behind. The black dots along the x-axis mark the time points where there is a significant one sample t-test against zero ($p < .05$).

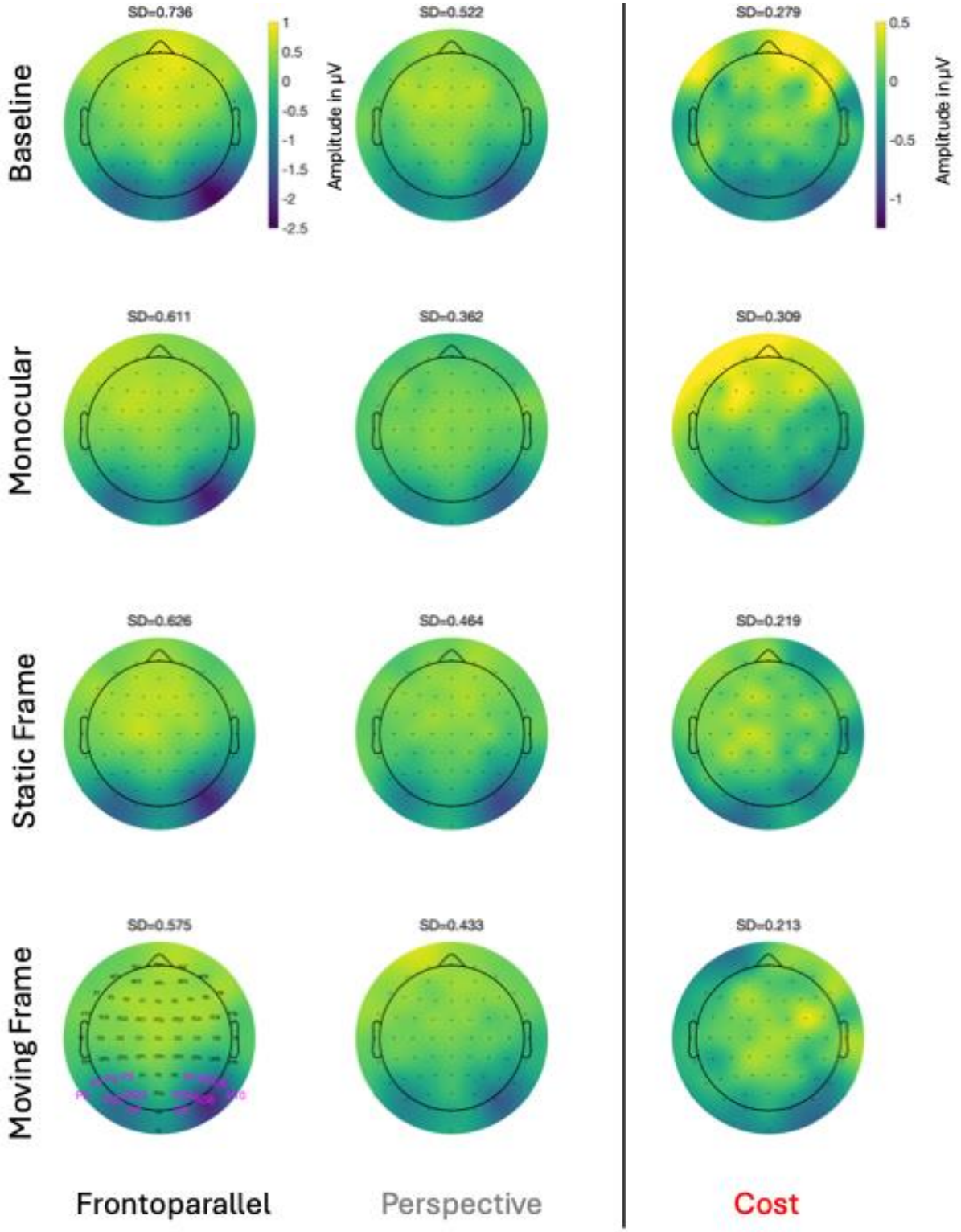

Figure 11. Topographic symmetry-asymmetry difference maps from the 300-600 ms window. The SPN appears as dark blue at posterior electrodes. The right column is the difference between frontoparallel and perspective SPNs. Here perspective cost appears as dark blue at posterior electrodes. SD above each topoplot refers to the standard deviation of amplitudes across the 64 electrodes. The 14 posterior electrodes used in all analysis are label in bottom left panel.

Figure 12 shows comparison of predicted and observed means, while Figure 13 shows distributions of individual amplitudes around these means.

Hypothesis 1 was supported. Amplitude was more negative for symmetrical than asymmetrical patterns in the frontoparallel conditions across all 4 blocks ($F(1,119) = 210.75$ $p < .001$, $\eta p^2 = .639$).

Hypothesis 2 was also supported. The SPN was stronger (more negative) in the Baseline frontoparallel condition compared to the Baseline perspective condition ($t(119) = -3.79$, $p < .001$, $d_z = -0.346$).

Hypothesis 3 was not supported. There was no significant difference between the perspective cost in Baseline and Monocular blocks ($t(119) = 0.35$, $p = .729$, $d_z = 0.032$); Baseline and Static frame blocks ($t(119) = -0.53$, $p = .595$, $d_z = -0.049$); Baseline and Moving frame blocks ($t(119) = -0.67$, $p = .507$, $d_z = -0.061$) or Static frame and Moving frame blocks ($t(119) = -0.13$ $p = .901$, $d_z = -0.011$).

Hypothesis 4 was not supported. Perspective cost in the Moving frame block was -0.24 microvolts. This was significantly *below* 0 ($t(119) = -2.19$, $p = .015$, $d_z = -0.200$), and not significantly *above* -0.35 ($t(119) = 1.07$, $p = .142$, $d_z = 0.098$). In other words, there was a small but significant perspective cost in the Moving frame block, contrary to our predictions.

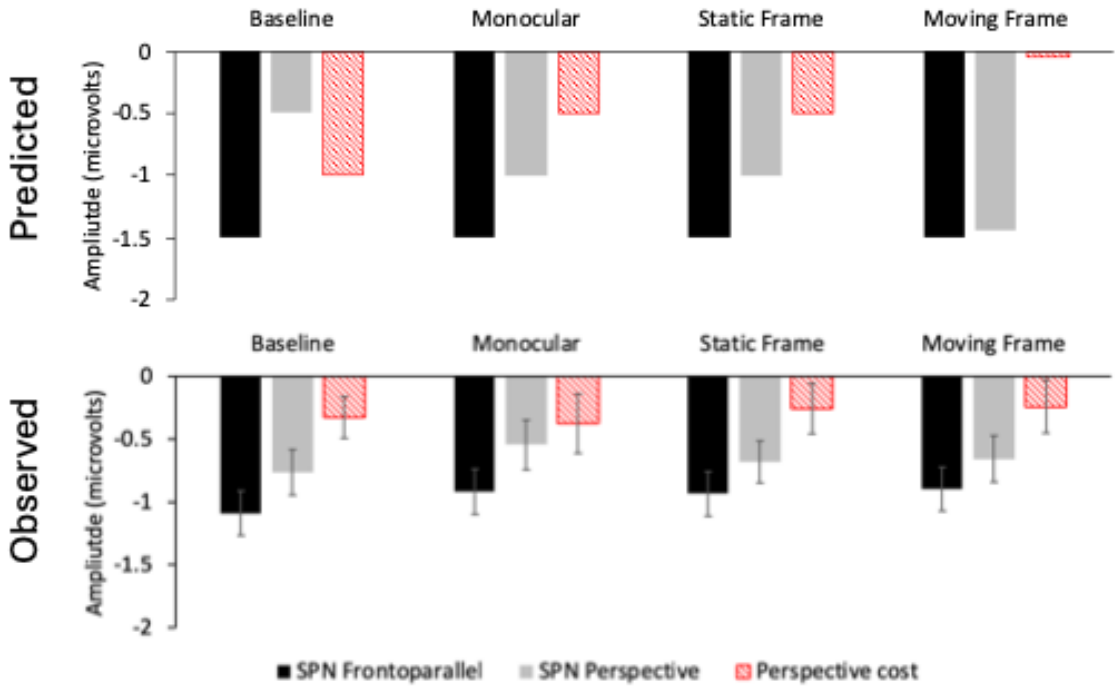

Figure 12. Predicted vs Observed results. The predicted results are also shown in Figure 3. The observed results are shown below for comparison. Contrary to predictions, perspective cost was similar in all blocks (red bars comparable). Error bars = 95% CI. All means were significantly < 0 ($p < 0.05$).

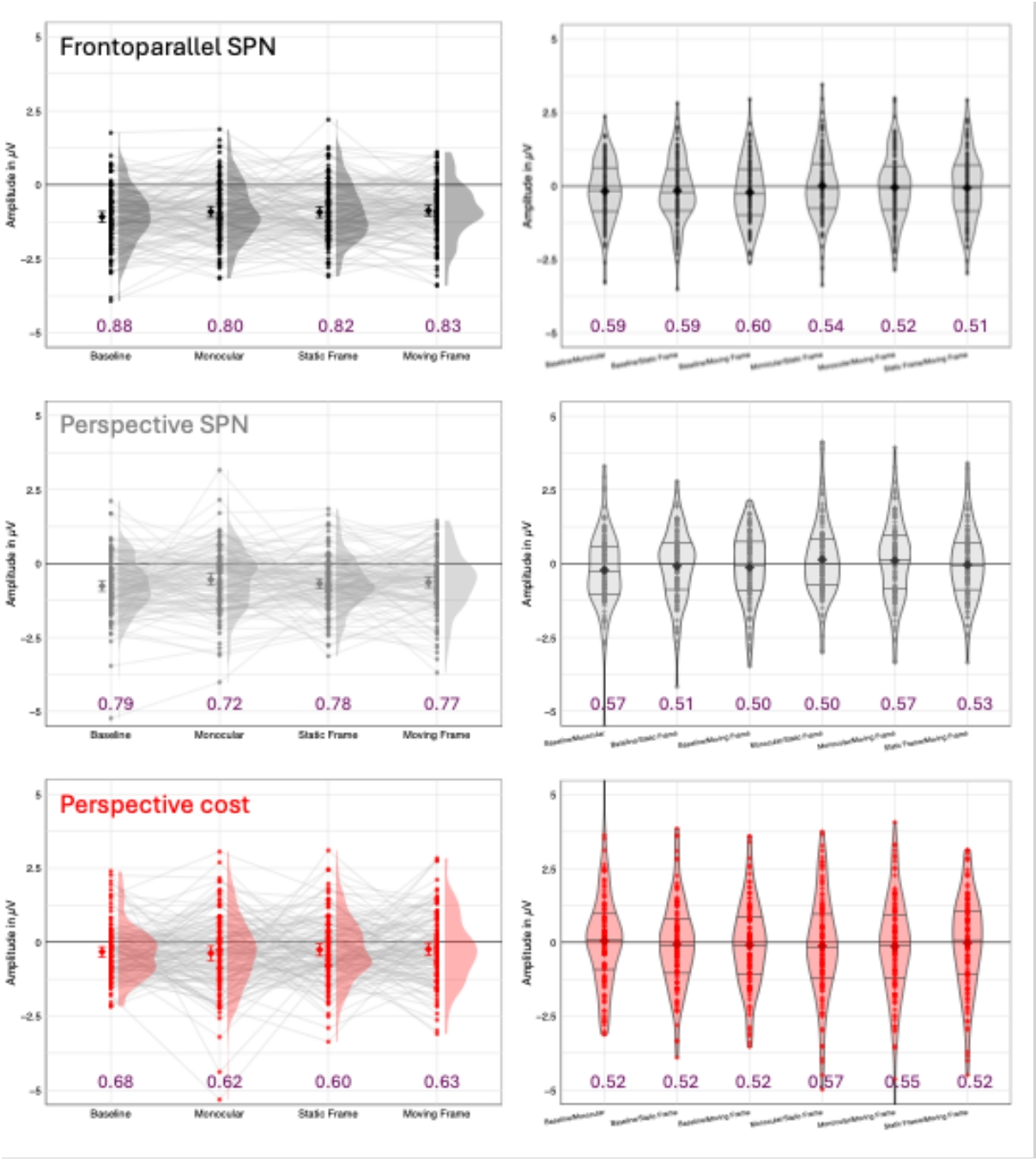

Figure 13. Scatterplots of ERP results (left) and distribution of pairwise differences (right). Conventions are the same as Figure 8. Purple numbers indicate the proportion of participants with an effect in the same direction as the group. Any proportions >= 0.6 are significantly > 0.5 according to non-parametric binomial tests ($p < 0.05$).

Additional exploratory analyses

To check whether Block order significantly influenced perspective cost, we ran an additional mixed ANOVA. There was no main effect of Block order on perspective cost ($F(3, 288) = 0.39$, $p = .759$, $\eta p^2 = .004$) and no interaction between Block and Block order ($F(69, 288) = 0.98$, $p = .538$, $\eta p^2 = .189$).

Next, we applied the equivalence testing approach to confirm the absence of the four expected pairwise differences listed under Hypothesis 3. These pairwise differences were all significantly less than 0.35 microvolts (Baseline vs Monocular, $t(119) = 2.76$ $p = .003$, $d_z = 0.252$; Baseline vs. Static frame, $t(119) = 2.13$, $p = .018$, $d_z = 0.194$; Baseline vs. Moving Frame, $t(119) = 1.97$, $p = .025$, $d_z = 0.180$; Static frame vs. Moving frame, $t(119) = 2.30$, $p = .012$, $d_z = 0.209$).

Figure 13 shows the two pairwise differences which did not feature in our pre-registered predictions, namely, Monocular vs. Static Frame and Monocular vs. Moving frame. These differences were not significantly different to 0 (Monocular vs. Static Frame $t(119) = -0.77$, $p = 0.445$, $d_z = -0.07$; Monocular vs. Moving Frame, $t(119) = -0.906$, $p = 0.367$, $d_z = -0.083$) but neither were they significantly less than less than 0.35 microvolts (Monocular vs. Static Frame $t(119) = 1.462$, $p = 0.073$, $d = 0.133$; Monocular vs. Moving Frame, $t(119) = 1.383$, $p = 0.085$, $d_z = 0.126$).

Finally, we explored correlations between individual SPN amplitudes, perspective cost, and behavioural performance. The Spearman's rho correlation matrix in shown in Figure 14. We used Spearman's Rho due to non-normal distribution of residuals, although a very similar matrix obtains when Pearson's r was used instead. With our sample of 120, we can expect to detect many moderate correlations (e.g. $r = 0.25$ or $rho = 0.26$, power = 0.8, alpha = 0.05, two-tailed). Scatterplots associated with this heatmap are shown in Supplementary materials. Participants who had a large SPN in one condition tended to have a larger SPN in the other conditions (red cells in top left, Figure 14A). Unsurprisingly, participants who had a larger frontoparallel SPN tend to have a larger perspective cost, while those with a larger perspective SPN tended to have a smaller perspective cost (alternating red and blue steps near diagonal, Figure 14B). There was little evidence that perspective cost correlated between blocks (Figure 14C). Those who performed well in one block tended to do so on other blocks (Figure 14D). However, there was little correlation between behavioural performance and

ERP signals (just 1/48 significant effects, rho = 0.186, p = .042, uncorrected for multiple comparisons, Figure 14E).

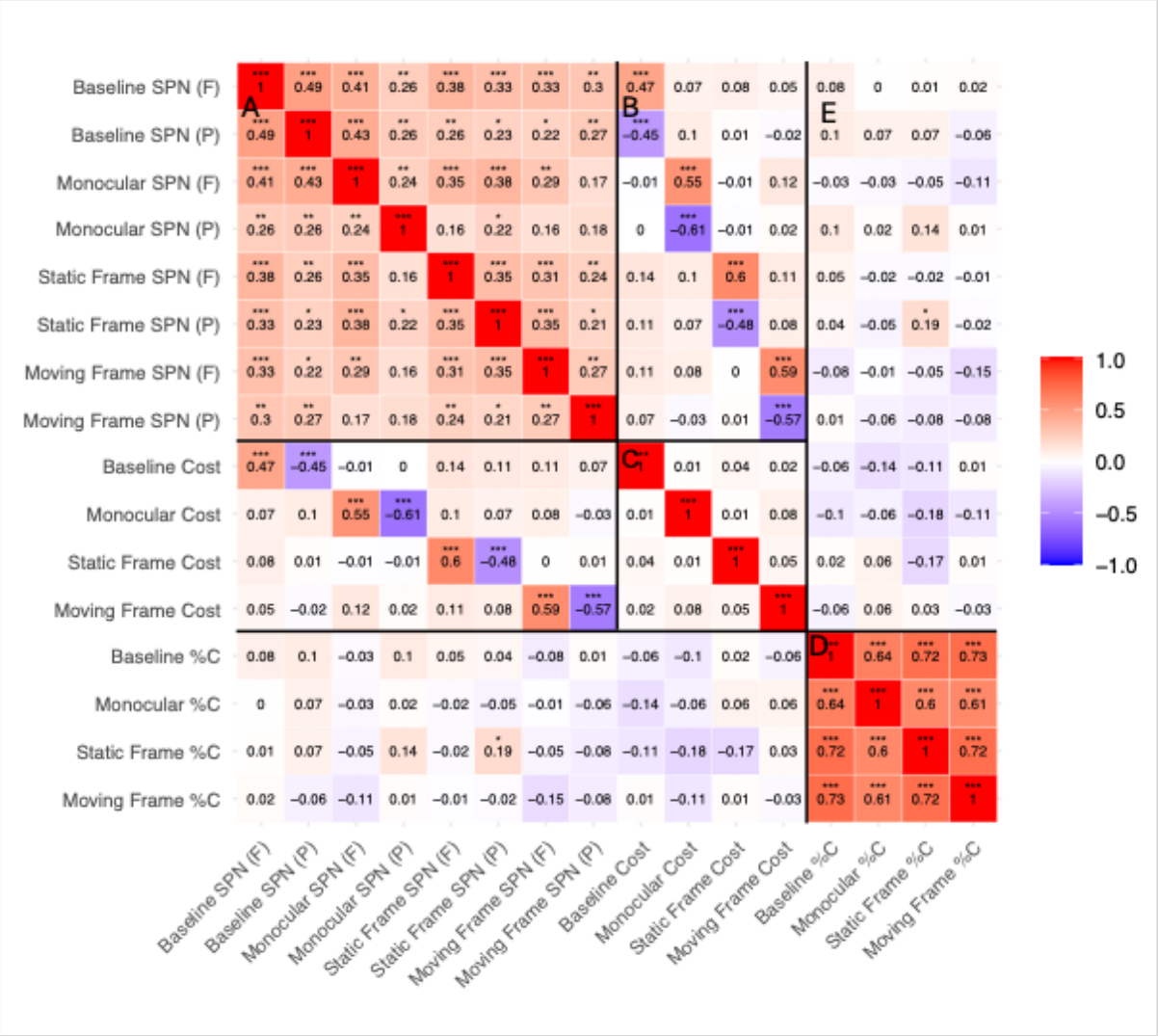

Figure 14. Spearman's Rho Correlation matrix of ERP and behavioural data. Blue cells indicate negative relationships, red indicate positive relationships. Zones A, B, C, D and E are interpreted in text. * $p < 0.05$, ** $p < 0.01$, *** $p < 0.001$.

Discussion

Previous research has found an SPN perspective cost during colour discrimination tasks (Figure 2). We reasoned that enhancing visual depth cues might reduce this SPN perspective cost. After all, shape constancy is subjectively effortless under naturalistic viewing conditions. However, contrary to our predictions, SPN perspective cost was ubiquitous and similar during Baseline, Monocular, Static frame and Moving frame blocks. We conclude that these visual cues are not sufficient to reduce perspective cost.

Reflectional symmetry is not the only regular arrangement that generates and SPNs (Rampone & Makin, 2020; Martinovic et al., 2011). If one considers our perspective stimuli as 2D images only, the 'symmetrical' ones were still more regular than the asymmetrical ones. The 'symmetrical' stimuli contained long implicit lines, with some fanning out from a single point and others almost vertical and parallel (Figure 5). Can we be sure that this 2D fan-and-vertical line regularity alone did not account for the SPN in the so-called 'perspective' conditions? It is possible that the 2D regularity in the 'perspective' conditions was less salient than the 2D reflectional symmetry frontoparallel conditions. This salience difference could explain the observed 'perspective cost.' However, we think this explanation is unlikely. As noted in the supplementary materials, participants spontaneously perceived the 3D perceptual interpretation of the stimuli.

A key assumption in Makin et al. (2015) was that participants achieved perfect extraretinal representation when focusing on regularity. This conclusion was based on the finding that the SPN was nearly identical for frontoparallel, and perspective displays during regularity discrimination (Figure 2B). However, there is another explanation for this SPN equivalence during regularity discrimination. On perspective trials in Makin (2015), retinal symmetry was hardly disrupted at all near the vertical axis. It could be that when participants attended to regularity, they focused spatial attention on the region near the vertical axis, which is known to be especially important for symmetry detection (Dakin & Herbert, 1998, Wainwright, 2020). Symmetry in the putatively attended region was very similar for frontoparallel and perspective displays, and this could explain the similar SPN. Conversely, when participants attended to luminance, they may have focused spatial attention on the whole stimulus area, not just the region near the vertical axis. Symmetry in the larger attended region was reduced for perspective displays, and this could explain the reduced SPN. This consideration highlights the importance of using perspective displays that eliminate symmetry in the axis region.

A future research priority is to determine whether perfect extraretinal representations of planar symmetry are ever constructed, even during regularity discrimination. Indeed, Karakashevska and Makin (forthcoming) reported SPN perspective cost during regularity discrimination with dot patterns like those in the current study. It nevertheless remains possible that some very strong visual manipulation could abolish SPN perspective cost. For instance, we could physically turn the monitor so that all visual and

cognitive cues imply the presence of a real slanted surface. Alternatively, virtual reality offers opportunities for interesting manipulations with rich scenes. However, at present, it is unclear whether there *any* scenarios in which the extrastriate symmetry network comes to treat frontoparallel and perspective symmetry as the same thing.

Conclusion

When attending to element luminance, the brain still responds to symmetry. However, the response to frontoparallel symmetry is stronger than the response to perspective symmetry. Adding visual cues that aid 3D interpretation does not reduce this perspective cost substantially.

Data and code availability

The pre-registration of this report, all saved images and the stimulus construction algorithm are available, along with EEG data at various levels of granularity, are available on OSF (https://osf.io/9pmrh/). This is also project 44 in the complete Liverpool SPN catalogue. (https://osf.io/2sncj/).

Acknowledgements

This study was supported by an ESRC doctoral studentship to EK and ERSC grant ES/S014691/1 awarded to AM and MB.

Conflict of interest

The authors declare no conflict of interest.

CRediT statement

Conceptualization: EK, AM, MB

Data curation and analysis: EK

Funding Acquisition: EK, AM

Writing –original draft: EK

Writing –review & editing: AM, EK, MB

Question	Hypothesis	Sampling plan	Analysis Plan	Rationale for deciding the sensitivity of the test for confirming or disconfirming the hypothesis	Interpretation given different outcomes	Theory that could be shown wrong by the outcomes
Which visual cues facilitate extraretinal representation of planar symmetrical dot patterns?	**Hypothesis 1** In the frontoparallel conditions amplitude will be lower for symmetry compared to asymmetry at posterior electrodes between 300 and 600 ms post stimulus onset. We are confident that this SPN will be observed in the new experiment, given the number of previous studies with similar stimuli (Makin, 2022).	We will collect 120 participants with normal or corrected-to-normal vision. This allows all possible 24 combinations of block orders to be presented 5 times.	We will run a 2 Regularity (Symmetry, Asymmetry) X 4 Block (Baseline, Monocular, Static frame, Moving frame) repeated measures ANOVA. We expect that Hypothesis 1 will be confirmed by a strong main effect of Regularity.	The sample size of 120 was chosen to detect smaller effects and is thus adequate to detect the main effect of Regularity in the frontoparallel conditions, which is likely to be large. Based on an unpublished study with similar stimuli and task (Karakashevska et al. forthcoming), we estimate the SPN in frontoparallel conditions will be 1.14 microvolts, and effect size will be η_p^2 = 0.528. Even assuming true effect size is half this, power approaches 1.”	We are confident that the expected SPN in the frontoparallel conditions will be observed given the number of previous studies with similar stimuli (Makin, 2022). If this claim is not supported by the data, we will conclude that something in the experiment went wrong.	The brain is not sensitive to retinal symmetry during luminance discrimination tasks (not very likely).
	Hypothesis 2 In the Baseline block, SPN will be much larger (more negative) for frontoparallel than perspective stimuli. In other words, perspective cost will be substantial in the	As above.	SPNs will be extracted with pre-registered pipeline, and a priori spatio-temporal windows. We will compute the difference between frontoparallel and	We define a small but meaningful SPN difference as 0.35 microvolts. Makin et al (2022) estimated that a typical SPN modulation of 0.35	Based on Makin et al. (2015) and Karakashevska et al. (forthcoming) we are confident that we will observe a perspective cost in the baseline block. If the data does not	The brain codes extraretinal symmetry automatically, even in the absence of facilitatory visual cues (not very likely)

	baseline block (Makin, 2015).		perspective SPNs in the baseline block. We will use a paired samples t test to confirm this (two-tailed).	microvolts has a Cohen's dz of 0.34. N=120 provides 91% chance of finding a significant pairwise difference if true dz is 0.34 (alpha = 0.02, two tailed). Power rises to 0.95 if one-tailed tests are used. This would be justifiable, given that we have directional hypotheses. However, our study is adequately powered (>0.9) whether one or two tailed tests are used.	support this claim, we will conclude that the brain is often sensitive to extra-retinal symmetry when discriminating luminance, and previous observations of perspective cost during luminance discrimination may not be reliable.	

	Hypothesis 3 Testing Hypothesis 3 is the main aim of our experiment. Hypothesis 3 states that perspective cost will be will differ between the four blocks (Red bars in Figure 3). This can be stated as four predicted pairwise differences: a) Perspective cost will be reduced in the Monocular viewing block (as compared to Baseline). b) Perspective cost will be reduced in the Static frame block (as compared to Baseline). c) Perspective cost will be reduced in the Moving frame block (as compared to Baseline). d) Perspective cost will be reduced in the Moving frame block (as compared to Static frame block).	As above.	The dependant variable here will be perspective cost (frontoparallel SPN – perspective SPN). We will test the four predicted effects with paired samples t tests (two tailed), using Bonferroni correction for multiple comparisons (0.05/4 = 0.125).	N=120 gives 88% power for finding a significant difference if true dz = 0.34 (alpha = 0.0125, two tailed).	It is possible that perspective cost is similar in all four blocks. In this case we would conclude that none of cue manipulations are sufficient for extraretinal symmetry representation during luminance discrimination.	The balance of retinal/extraretinal coding is always the same, whether our cues are present or not (possible but not likely).
	Hypothesis 4 We predict perspective cost will approximate zero in the Moving frame block. In other words,	As above.	For hypothesis 4 we will use a one-sided equivalence testing approach.	We will only conclude a perspective cost exists in a block if it is significantly more than zero, and not	If the Moving frame block does not abolish perspective cost, we will conclude that this cue is not sufficient	Moving frames are not sufficient to achieve automatic extraretinal

	we predict near-perfect frontoparallel-perspective SPN equivalence in the Moving frame block, and not in the other three blocks.		To confirm the presence of perspective cost (as expect in Baseline, Monocular and Static frame blocks), we will compare against zero with one-tailed one sample t test. Then to confirm the absence of perspective cost (as expected in the Moving frame block), we will compare against -0.35 microvolts one-tailed one sample t-tests.	significantly less than -0.35. We will only conclude a perspective cost is absent in a block if it is also significantly less than -0.35 microvolts (our a priori definition of a small effect). Power for the one-sided t tests used in these analyses = 0.95.	for achieving automatic extraretinal representation.	representation (possible).

Notes on terminology

- The Sustained posterior Negativity (SPN) is an ERP response to visual symmetry. It is the difference between waves generated by symmetrical and asymmetrical stimuli at posterior electrodes. A large SPN is one which falls a long way below zero.
- 'Extraretinal' in another word for 'allocentric', 'post-constancy', object level or 'view-invariant'.
- We use the word 'perspective' to refer to images in which dot pattern is depicted as if viewed from an angle. These stimuli combine 60-degree slant and 15-degree tilt.
- We will referrer the different conditions in the experiment as blocks rather than cues since monocular viewing involves removal of cue conflict rather than an additional cue.

References

Allison, R. S., & Howard, I. P. (2000). Temporal dependencies in resolving monocular and binocular cue conflict in slant perception. Vision Research, 40(14), 1869-1885. https://doi.org/10.1016/S0042-6989(00)00034-1

Barlow, H. B., & Reeves, B. C. (1979). Versatility and absolute efficiency of detecting mirror symmetry in random dot displays. *Vision Research*, *19*(7), 783–793. https://doi.org/10.1016/0042-6989(79)90154-8

Bertamini, M., Silvanto, J., Norcia, A. M., Makin, A. D. J., & Wagemans, J. (2018). The neural basis of visual symmetry and its role in mid- and high-level visual processing. *Annals of the New York Academy of Sciences*, *1426*(1), 111–126. https://doi.org/10.1111/nyas.13667

Bertamini, M., Tyson-Carr, J., & Makin, A. D. J. (2022). Perspective slant makes symmetry harder to detect and less aesthetically appealing. *Symmetry*, *14*(3). https://doi.org/10.3390/sym14030475

Brookes, A., & Stevens, K. A. (1989). The analogy between stereo depth and brightness. Perception, 18(5), 601-614.

Cattaneo, Z. (2017). The neural basis of mirror symmetry detection: a review. *Journal of Cognitive Psychology*, *29*(3), 259–268. https://doi.org/10.1080/20445911.2016.1271804

Cornilleau-Pérès, V., Wexler, M., Droulez, J., Marin, E., Miege, C., & Bourdoncle, B. (2002). Visual perception of planar orientation: dominance of static depth cues over motion cues. Vision research, 42(11), 1403-1412. https://doi.org/10.1016/S0042-6989(01)00298-X

Dakin, S. C., & Herbert, A. M. (1998). The spatial region of integration for visual symmetry detection. *Proceedings. Biological Sciences*, *265*(1397), 659–664. https://doi.org/10.1098/rspb.1998.0344

Farshchi, M., Kiba, A., & Sawada, T. (2021). Seeing our 3D world while only viewing contour-drawings. Plos one, 16(1), e0242581. https://doi.org/10.1371/journal.pone.0242581

Höfel, L., & Jacobsen, T. (2007). Electrophysiological indices of processing symmetry and aesthetics: A result of judgment categorization or judgment report? *Journal of Psychophysiology*, *21*(1), 9–21. https://doi.org/10.1027/0269-8803.21.1.9

Hoffman, D. (1998). *Visual Intelligence: How we create what we see*. W.W. Norton & Company.

Jacobsen, T., & Höfel, L. (2003). Descriptive and evaluative judgment processes: Behavioral and electrophysiological indices of processing symmetry and aesthetics. *Cognitive Affective & Behavioral Neuroscience*, *3*(4), 289–299. https://doi.org/10.3758/CABN.3.4.289

Karakashevska, E., Rampone, G., Tyson-Carr, J., Makin, A. D. J., & Bertamini, M. (2021). Neural responses to reflection symmetry for shapes defined by binocular disparity, and for shapes perceived as regions of background. *Neuropsychologia*, *163*, 108064. https://doi.org/10.1016/j.neuropsychologia.2021.108064

Keefe, B. D., Gouws, A. D., Sheldon, A. A., Vernon, R. J. W., Lawrence, S. J. D., McKeefry, D. J., Wade, A. R., & Morland, A. B. (2018). Emergence of symmetry selectivity in the visual areas of the human brain: fMRI responses to symmetry presented in both frontoparallel and slanted planes. *Human Brain Mapping*, *39*(10), 3813–3826. https://doi.org/10.1002/hbm.24211

Koffka. (1935). *Principles of Gestalt Psychology*. Harcourt, Brace & Company.

Kohler, P. J., Clarke, A., Yakovleva, A., Liu, Y., & Norcia, A. M. (2016). Representation of maximally regular textures in human visual cortex. *The Journal of Neuroscience*, *36*(3), 714–729. https://doi.org/10.1523/JNEUROSCI.2962-15.2016

Koning, A., & Wagemans, J. (2009). Detection of symmetry and repetition in one and two objects. *Experimental Psychology*, *56*(1), 5–17. https://doi.org/10.1027/1618-3169.56.1.5

Lakens, D., Scheel, A. M., & Isager, P. M. (2018). Equivalence testing for psychological research: A tutorial. Advances in Methods and Practices in Psychological Science, 1(2), 259-269.

Li, A., & Zaidi, Q. (2004). Three-dimensional shape from non-homogeneous textures: Carved and stretched surfaces. Journal of Vision, 4(10), 3-3. https://doi.org/10.1167/4.10.3

Locher, P. J., & Smets, G. (1992). The influence of stimulus dimensionality and viewing orientation on detection of symmetry in dot patterns. *Bulletin of the Psychonomic Society*, *30*(1). https://doi.org/10.3758/BF03330392

Makin, A. D. J., Rampone, G., & Bertamini, M. (2015). Conditions for view invariance in the neural response to symmetry. *Psychophysiology*, *52*(4), 532–543. https://doi.org/DOI: 10.1111/psyp.12365

Makin, A. D. J., Rampone, G., Morris, A., & Bertamini, M. (2020). The formation of symmetrical gestalts is task independent, but can be enhanced by active regularity discrimination. *Journal of Cognitive Neuroscience*, *32*(2), 353–366. https://doi.org/10.1162/jocn_a_01485

Makin, A. D. J., Rampone, G., Pecchinenda, A., & Bertamini, M. (2013). Electrophysiological responses to visuospatial regularity. *Psychophysiology*, *50*, 1045–1055. https://doi.org/10.1111/psyp.12082

Makin, A. D. J., Roccato, M., Karakashevska, E., Tyson-Carr, J., & Bertamini, M. (2023). Symmetry Perception and Psychedelic Experience. *Symmetry*, *15*(7), 1340. https://doi.org/10.3390/sym15071340

Makin, A. D. J., Tyson-Carr, J., Rampone, G., Derpsch, Y., Wright, D., & Bertamini, M. (2022). Meta Research: Lessons from a catalogue of 6674 brain recordings. *ELife*, *11*, e66388. https://doi.org/DOI: https://doi.org/10.7554/eLife.66388

Makin, A. D. J., Wright, D., Rampone, G., Palumbo, L., Guest, M., Sheehan, R., Cleaver, H., & Bertamini, M. (2016). An electrophysiological index of perceptual goodness. *Cerebral Cortex*, *26*, 4416–4434. https://doi.org/doi: 10.1093/cercor/bhw255

Martinovic, J., Mordal, J., & Wuerger, S. M. (2011). Event-related potentials reveal an early advantage for luminance contours in the processing of objects. *Journal of Vision*, *11*(7). https://doi.org/1 10.1167/11.7.1

Mognon, A., Jovicich, J., Bruzzone, L., & Buiatti, M. (2011). ADJUST: An automatic EEG artifact detector based on the joint use of spatial and temporal features. Psychophysiology, 48(2), 229-240. https://doi.org/10.1111/j.1469-8986.2010.01061.x

Møller, A. P., & Thornhill, R. (1998). Bilateral symmetry and sexual selection: A meta-analysis. *American Naturalist*, *151*(2), 174–192. https://doi.org/10.1086/286110

Norman, J. F., Payton, S. M., Long, J. R., & Hawkes, L. M. (2004). Aging and the perception of biological motion. Psychology and aging, 19(1), 219. https://doi.org/10.1037/0882-7974.19.1.219

Peirce, J. W. (2007). PsychoPy - Psychophysics software in Python. *Journal of Neuroscience Methods*, *162*(1–2), 8–13. https://doi.org/10.1016/j.jneumeth.2006.11.017

Rampone, G., Makin, A. D. J., Tatlidil, S., & Bertamini, M. (2019). Representation of symmetry in the extrastriate visual cortex from temporal integration of parts: An EEG/ERP study. *NeuroImage*, *193*, 214–230. https://doi.org/10.1016/J.NEUROIMAGE.2019.03.007

Rampone, G., & Makin, A. D. J. (2020). Electrophysiological responses to regularity show specificity to global form: The case of Glass patterns. *European Journal of Neuroscience*, *52*(3), 3032–3046. https://doi.org/10.1111/ejn.14709

Sambul, A. M., Murayama, N., & Igasaki, T. (2013). Event-related potential study on image-symmetry discrimination in the human brain. *2013 35th Annual International Conference of the IEEE Engineering in Medicine and Biology Society (EMBC)*, *2013*, 5938–5941. https://doi.org/10.1109/EMBC.2013.6610904

Sasaki, Y., Vanduffel, W., Knutsen, T., Tyler, C. W., & Tootell, R. (2005). Symmetry activates extrastriate visual cortex in human and nonhuman primates. *Proceedings of the National Academy of Sciences of the United States of America*, *102*(8), 3159–3163. https://doi.org/10.1073/pnas.0500319102

Sawada, T., & Pizlo, Z. (2008). Detection of skewed symmetry. *Journal of Vision*, *8*(5), 1–18. https://doi.org/10.1167/8.5.14.

Sawada, T., & Farshchi, M. (2022). Visual detection of 3D mirror-symmetry and 3D rotational-symmetry. Visual Cognition, 30(8), 546-563. https://doi.org/10.1080/13506285.2022.2139314

Szlyk, J. P., Rock, I., & Fisher, C. B. (1995). Level of processing in the perception of symmetrical forms viewed from different angles. *Spatial Vision*, *9*(1), 139–150. https://doi.org/10.1163/156856895x00151

Thouless, R. H. (1933). Phenomenal regression to the real object [2]. In *Nature* (Vol. 131, Issue 3311, pp. 261–263). https://doi.org/10.1038/131544b0

Treder, M. S. (2010). Behind the looking glass: A review on human symmetry perception. *Symmetry*, *2*, 1510–1543. https://doi.org/10.3390/sym2031510

Treue, S., & Maunsell, J. H. (1996). Attentional modulation of visual motion processing in cortical areas MT and MST. Nature, 382(6591), 539-541. https://doi.org/10.1038/382539a0

Tyler, C. W., Baseler, H. A., Kontsevich, L. L., Likova, L. T., Wade, A. R., & Wandell, B. A. (2005). Predominantly extra-retinotopic cortical response to pattern symmetry. *NeuroImage*, *24*(2), 306–314. https://doi.org/10.1016/j.neuroimage.2004.09.018

Tyson-Carr, J., Bertamini, M., Rampone, G., & Makin, A. D. J. (2021). Source dipole analysis reveals a new brain response to visual symmetry. *Scientific Reports*, *11*(1). https://doi.org/10.1038/s41598-020-79457-x

van der Vloed, G., Csathó, A., & van der Helm, P. A. (2005). Symmetry and repetition in perspective. *Acta Psychologica*, *120*(1), 74–92. https://doi.org/10.1016/j.actpsy.2005.03.006

Van Meel, C., Baeck, A., Gillebert, C. R., Wagemans, J., & Op de Beeck, H. P. (2019). The representation of symmetry in multi-voxel response patterns and functional connectivity throughout the ventral visual stream. *NeuroImage*, *191*, 216–224. https://doi.org/10.1016/j.neuroimage.2019.02.030

Vishwanath, D., & Hibbard, P. B. (2013). Seeing in 3-D with just one eye: Stereopsis without binocular vision. Psychological science, 24(9), 1673-1685. https://doi.org/10.1177/0956797613477867

Wainwright, J. B., Scott-Samuel, N. E., & Cuthill, I. C. (2020). Overcoming the detectability costs of symmetrical coloration. *Proceedings of the Royal Society B. 287: 20192664.* https://doi.org/10.1098/rspb.2019.2664

Wagemans, J. (1993). Skewed symmetry: A nonaccidental property used to perceive visual forms. *Journal of Experimental Psychology: Human Perception and Performance*, *19*(2), 364–380. https://doi.org/10.1037/0096-1523.19.2.364

Wagemans, J., Elder, J. H., Kubovy, M., Palmer, S. E., Peterson, M. A., Singh, M., & von der Heydt, R. (2012). A century of Gestalt psychology in visual perception: I. Perceptual grouping and figure–ground organization. *Psychological Bulletin*, *138*(6), 1172–1217. https://doi.org/10.1037/a0029333

Welchman, A. E. (2016). The human brain in depth: how we see in 3D. Annual review of vision science, 2, 345-376. https://doi.org/10.1146/annurev-vision-111815-114605